Static and Dynamic Analysis of a Rod-Fastened Rotor

Dr. N. Wagner, Dr. R. Helfrich
(INTES GmbH, Germany)

Abstract

A rod-fastened rotor is generally comprised of a series of discs clamped together by several tie rods uniformly distributed on the pitch circle diameter. The contact states of the contact interfaces clearly depend on the pre-tightening forces during the assembly process and additional operational loads. It turns out that jointed structures are inherently afflicted with uncertainties. For reasons of simplification, contacts are often replaced by multi-point constraints in the beginning of a finite element study. However, this approach overestimates the size of the corresponding glued areas and yields a comparatively stiff system behavior.

In this study, a two-step approach is established to cope with these uncertainties. The first step is a contact analysis which considers the different loads of the mounting situation and final operating conditions. Based on the results from the previous contact analysis, only active contacts are replaced by linear multipoint constraints. Moreover, a different treatment of normal and tangential directions of frictional contacts is available in order to mimic a realistic behaviour.

The second step comprises of three different analysis procedures. A static procedure is used to establish additional matrices due to rotation. Herein, the influence of the pre-stressed rods on the geometric stiffness matrix is neglected. The cyclic symmetric structure of the underlying rod-fastened rotor requires a treatment in the co-rotating reference system, where the geometric and centrifugal stiffness matrices are considered to compute the real mode shapes. Afterwards, the system is projected onto its modal subspace in order to compute the complex eigenfrequencies of the reduced-order model for a wide variety of rotational speeds.

An example similar to the literature is used to demonstrate the procedure using the commercial finite element package PERMAS. A comparison between the eigenfrequencies of a classically tied assembly and the new approach illustrates the paramount importance of an appropriate modeling of interfaces in jointed structures.

1. Introduction

An area of increasing importance over recent years has been the consideration of pre-stress effects on the dynamic behaviour of structures such as laminated rotors [6] and tie-rod/tie-bolt rotors [5,10,23]. Three different finite element beam models for laminated rotor cores in electrical machines are analysed and validated by comparing the first non-rotating natural frequencies under free-free support conditions with experimental results of a modal analysis for nine different rotors in [Santos2013]. Spindles are the most important components of machine tools. The influence of the press fit on the dynamic behaviour of a rotor shaft assembly is discussed in [1, 2]. Interference fits can be calculated in two different ways in PERMAS; by a contact analysis and a newly developed method, where a permanent coupling is used. Dynamic characteristics of joints in aero-engine rotor systems are analysed in [13]. The steady-state thermo-mechanical analysis of a four-disc rod fastened turbine rotor is examined in [25].A rod-fastening rotor supported by ball bearings is discussed in [18]. The identification of constitutive properties of a laminated rotor at rest are investigated in [7, 8]. Centrifugal effects on a prestressed laminated rotor are analyzed in [9]. Uncertainties in rotor dynamic analyses are mentioned in [17]. The effect of core stiffness on critical speeds is studied in [14]. Beam finite element models [7, 8, 12, 17, 24] are used in almost all of the early publications, whereas nowadays solid elements are used in [3, 11, 20, 21, 22] and the current study. Bolted rotors with curvic couplings are analysed under various viewpoints, such as stress distribution, contact status, and tightening method to achieve a uniform clamp force in a series of papers [20, 21, 22].

2. Example

The finite element model (Fig. 1) of the rod-fastened rotor is based on a recent example used in [3]. It consists of six discs, an after shaft, a forward shaft and twelve 12 tie rods which are uniformly distributed on the pitch circle diameter. The rotor is elastically supported by two isotropic bearings at both ends of the shaft. However, the elastic bearings are replaced by fixed supports in the numerical studies, for simplicity. The finite element model consists of 206940 hexahedral, 25224 pentahedral elements and 297179 nodes. 23 contacts and 12 pretension definitions are contained in the model. A constant friction coefficient $\mu=0.1$ is used.

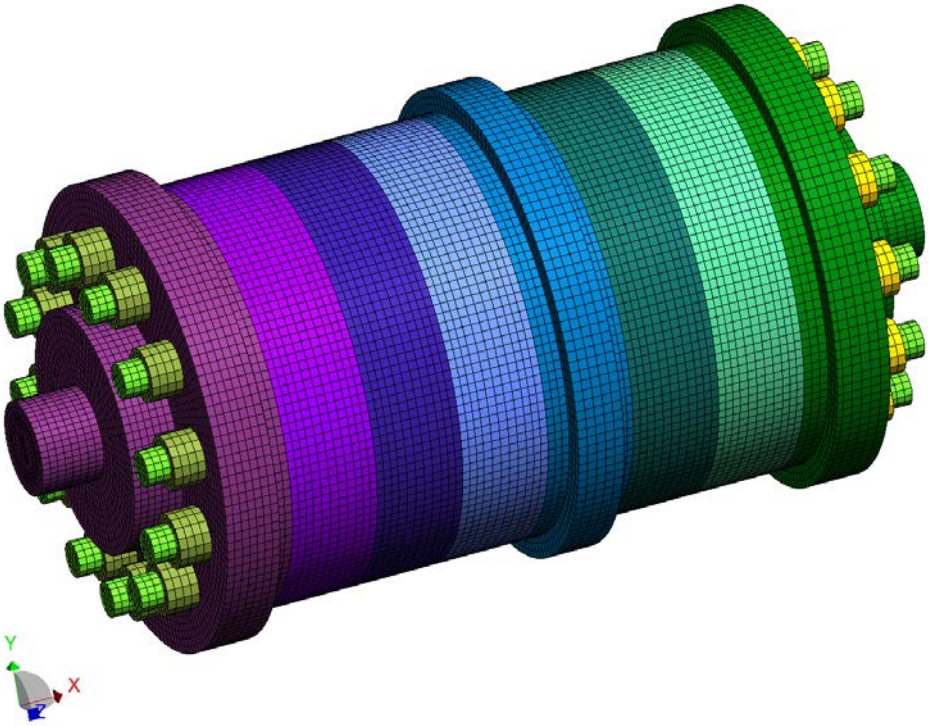

Figure 1: Finite element model of the rod-fastened rotor.

Several surface to surfnode contacts are defined between consecutive discs and support discs. A uniform pre-tightening force is applied to all tie rods. The first step is a static analysis. Contact and pretension definitions are supported by own wizards in VisPER (Visual PERMAS) [27]. Possible rigid body modes of the rod-fastened rotor assembly are detected by the so-called RBM assistant. As soon as the definition of contacts is complete, the RBM assistant may be used to define an elastic support of the contact bodies. In order to perform a subsequent modal analysis of the rotor, the contacts have to be linearized by using general multipoint constraints. Based on the results from the previous contact analysis, only active contacts are automatically replaced by linear multipoint constraints. Moreover, a different treatment of normal and tangential directions of frictional contacts is available in order to mimic a realistic behaviour. A further kind of fuzziness can be introduced here by using the current contact pressure value. Once the actual contact pressure exceeds a certain threshold a multipoint constraint is introduced. On that basis, a modal analysis is performed to compute the eigenfrequencies of the rotor at standstill. The influence of varying pretightening forces (10, 40 and 80 kN) on the real

eigenfrequencies of the rod-fastened rotor at standstill is illustrated in Fig. 2. The 24 local (bending) modes (2-25) are mainly dominated by the 12 tie-rods, whereas modes 1, 26, 27 and 28 are global modes of the rod-fastened rotor. Overall it turns out that the local modes are more sensitive to a variation of the pretension loads if the vertical distance between varicoloured points in the scatter plot is considered. So called caso files, which contain information of the contact status can be used in PERMAS to accelerate the contact iteration of subsequent runs [26, 28].

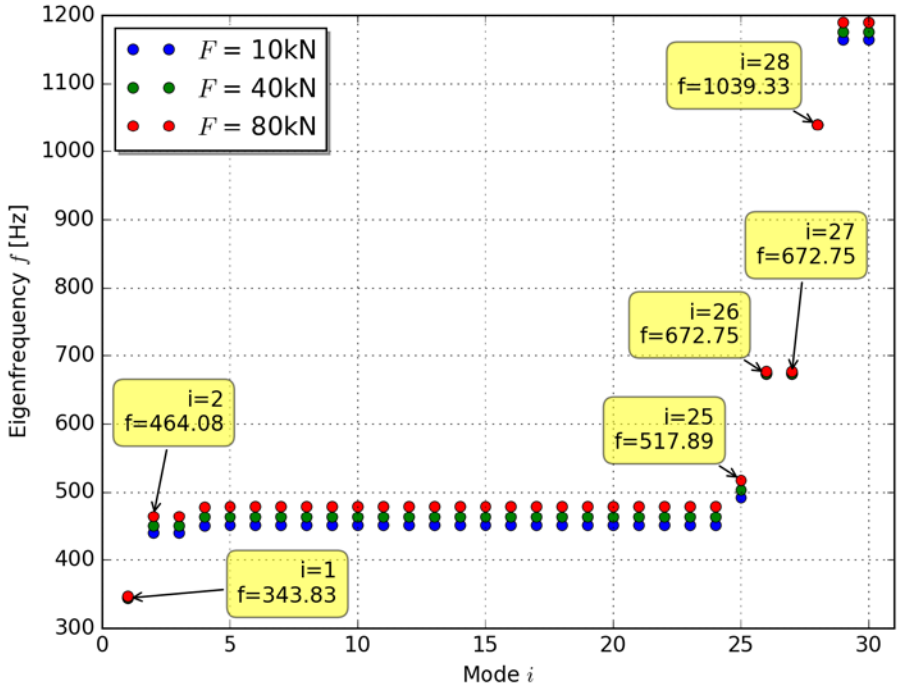

Figure 2: Eigenfrequencies for varying pretension forces.

Unbalanced pretightening forces induced by bolt loosening [11] of a single bolt or a group of bolts will certainly influence the static and dynamic behavior of the rotor. In this study, bolt failure is simulated by a low pretension force. Only a few modes are affected by the simulated bold failure as illustrated in Fig. 3. A maximum deviation of 12 % is observed. It would be interesting to find out, if this observation could be confirmed by experimental modal analysis.

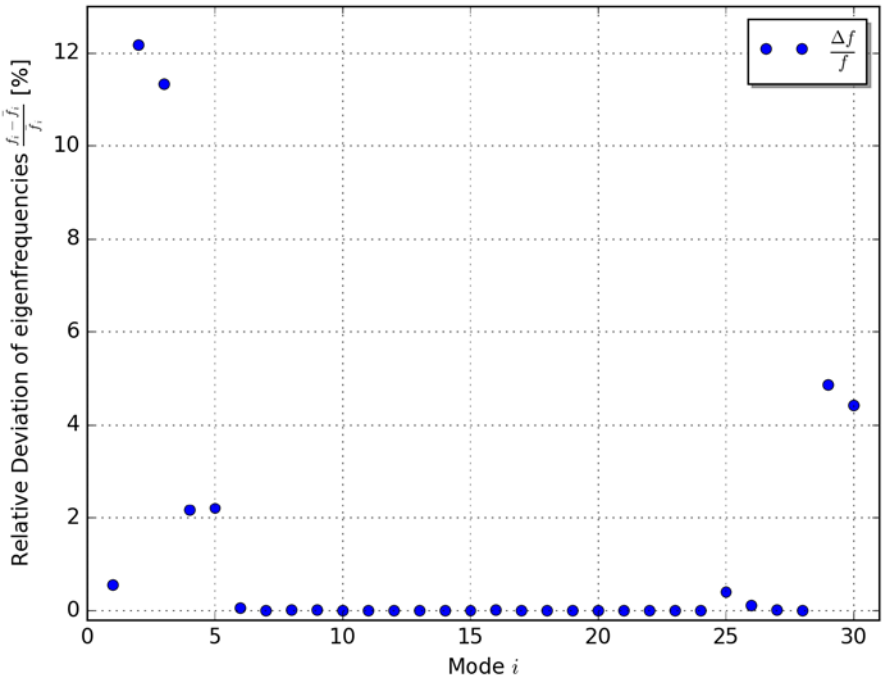

Figure 3: Eigenfrequency deviation between a rod-fastened rotor with uniform pretightening force (10 [kN]*) versus a system with a local loss of pretension load in one rod*

Secondly, the real eigenfrequencies are computed for a reference rotational speed taken into account additional matrices due to rotation, i.e. geometric and centrifugal stiffness. Since the rod-fastened rotor is a cyclic symmetric structure, we have to use a co-rotating reference system. The contribution of pretightening forces to the geometric stiffness matrix is neglected in this case. As a consequence, this means that only inertia loads are applied to the rod-fastened rotor to compute the geometrical stiffness matrix. Afterwards the real eigenvectors are used to transform and project the equations of motion into modal space. The complex eigenvalue problem is repeatedly solved for the reduced order model for different rotational speeds in consideration of the Coriolis matrix to obtain the Campbell diagram (Fig. 4) of the underlying system.

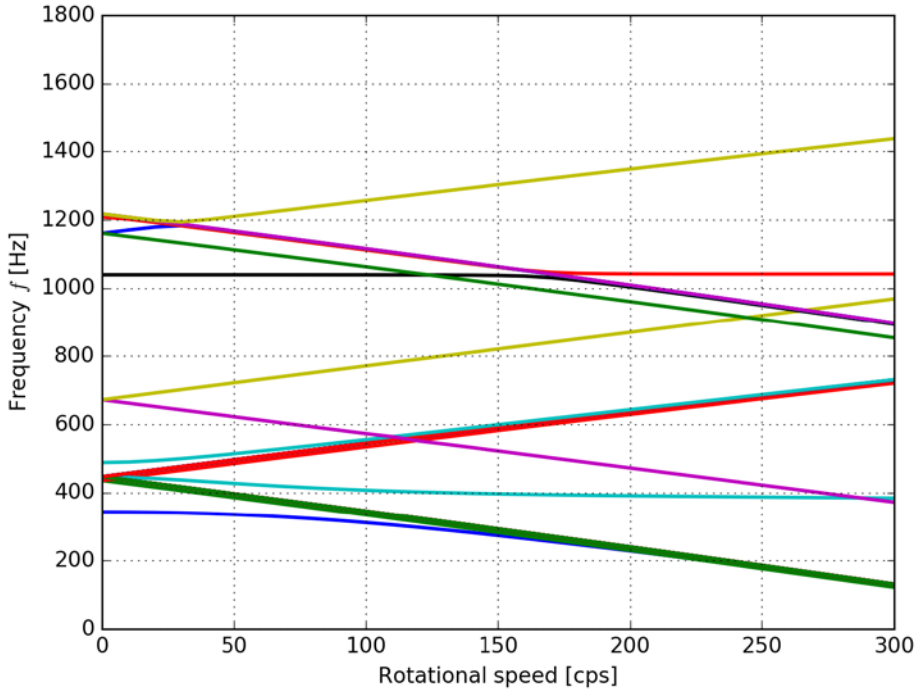

Figure 4: Campbell diagram of the rod-fastened rotor

3. Acknowledgements

The authors are grateful to Oguzhan Yalcin (Hochschule Esslingen) for providing us with the CAD model and our colleague Jens Müller for the finite element mesh of the rod-fastened rotor.

4. Conclusions

A two-step procedure for the computation of the dynamic behaviour of a rod-fastened rotor is presented. At the beginning a contact analysis is conducted under the consideration of pre-tightening loads. The usage of a detailed three-dimensional solid finite element model ensures a more realistic description of the contact zones of laminated rotors compared to simplified beam models. The proposed approach for treating rod-fastened rotors is able to predict the pretightening effect on the static and dynamic behaviour in the early development stage. In addition it is worthwile considering how the findings could be used to optimize prestressed structures.

5. References

[1] S.-Y. Chen, C. Kung, J.-C. Hsu (2011). Dynamic analysis of a rotary hollow shaft with hot-fit part using contact elements with friction, Transactions of the Canadian Society of Mechanical Engineering, Vol. 35, pp. 461—474

[2] S.-Y. Chen (2012). An equivalent direct modeling of a rotary shaft with hot-fit components using contact element modal analysis results, Computers and Mathematics with Applications, Vol. 64, pp. 1093--1099

[3] J. Gao, Q. Yuan, P. Li, Z. Feng, H. Zhang, Z. Lv (2012) Effects of bending moments and pre-tightening forces on the flexural stiffness of contact interfaces in rod-fastened rotors, Journal of Engineering for Gas Turbines and Power, Vol. 134

[4] M. Isa, J.E.T. Penny, S.D. Garvey (2000). The dynamics of bolted and laminated rotors, 18th International Modal Analysis Conference, pp. 867--872

[5] J. E. Jam, F. Meisami, N. G. Nia, (2011), Vibration analysis of tie-rod/tie-bolt rotors using FEM, International Journal of Engineering Science and Technology, Vol. 3, pp. 7292—7300

[6] Y.-C. Kim, K.-W. Kim (2006). Influence of lamination pressure upon the stiffness of laminated rotor, JSME International Journal Series C, Vol. 49, pp. 426--431

[7] G. Mogenier, N.-B. Thouraya, R. Dufour, L. Durantay, N. Barras (2011). Efficient model development for an assembled rotor of an induction motor using a condensed modal functional, Journal of Computational and Nonlinear Dynamics, Vol. 6

[8] G. Mogenier, N.-B. Thouraya, R. Dufour, L. Durantay, N. Barras (2010). Identification of constitutive properties of a laminated rotor at rest through a condensed modal functional, Mecanique & Industries, Vol. 11, pp. 309-326

[9] G. Mogenier, T. Baranger, R. Dufour, F. Besso, L. Durantay (2011). Nonlinear centrifugal effects on a prestressed laminated rotor, Vol. 46, pp. 1466--1491

[10] H. Peng, Z. Liu, G. Wang, M. Zhang, (2011), Rotor dynamic analysis of tie-bolt fastened rotor based on elastic-plastic contact, Proceedings of ASME Turbo Expo, June 6-10, Vancouver, British Columbia, Canada

[11] Z. Qin, Q. Han, F. Chu (2016). Bolt loosening at rotating joint interface and its influence on rotor dynamics, Engineering Failure Analysis, Vol. 59, pp. 456--466

[12] H. L. V. Santos, M. A. Luersen, C. A. Bavastri (2013). Experimental evaluation of numerical models to represent the stiffness of laminated rotor cores in electrical machines, Journal of Engineering Science and Technology, Vol. 8, pp. 457--471

[13] L. Shuguo, M. Yanhong, Z. Dayi, H. Jie (2012). Studies on dynamic characteristics of the joint in the aero-engine rotor system, Mechanical Systems and Signal Processing, Vol. 29, pp. 120—136

[14] S. Singhal, K. V. Singh, A. Hyder (2011). Effect of laminated core on rotor mode shape of large high speed induction motor, Electric Machines & Drives Conference, 15-18 May 2011, IEEE

[15] Z. Qin, Q. Han, F. Chu, (2016), Bolt loosening at rotating joint interface and its influence on rotor dynamics, Engineering Failure Analysis, Vol. 59, pp. 456—466

[16] K. Xia, Y. Sun, D. Hong, J. Guo, X. Kang (2016). Effects of contact interfaces on rotor dynamic characteristics of heavy-duty gas turbine generator set, Proceedings of 2016 IEEE, International Conference on Mechatronics and Automation, August 7-10, Harbin, China

[17] M. Yanhong, L. Zhichao, C. Meng, H. Jie (2013). Interval analysis of rotor dynamic response with uncertain parameters, Journal of Sound and Vibration, Vol. 332, pp. 3869--3880

[18] J. Yi, H. Liu, Yi Liu, M. Jing, (2015), Global nonlinear dynamic characteristics of rod-fastening rotor supported by ball bearings, Proc. IMechE Part K: J. Multibody Dynamics, Vol. 229, pp. 208-222

[19] Q. Yuan, J. Gao, P. Li (2014). Nonlinear Dynamics of the rod-fastened Jeffcott Rotor, Journal of Vibration and Acoustics, Vol. 136

[20] S. Yuan, Y. Zhang, Y. Zhang, X. Jiang (2010). Stress distribution and contact status analysis of a bolted rotor with curvic couplings. Proc. IMechE, Part C: J. Mechanical Engineering Science, Vol. 224, pp. 1815--1829

[21] S. Yuan, Y. Zhang, Y. Fan, Y. Zhang (2016). A method to achieve uniform clamp force in a bolted rotor with curvic couplings, Proc. IMechE Part E, J. Process Mechanical Engineering, Vol. 230, pp. 335-344

[22] S. Yuan, Y. Zhang, Y. Zhu (2015). Influence of thin-wall structure on stress distribution of curvic couplings, Journal of Theoretical and Applied Mechanics, Vol. 45, pp. 37--52

[23] Y. Zhang, Z. Du, L. Shi, S. Liu (2010). Determination of contact stiffness of rod-fastened rotors based on modal test and finite element analysis, Journal of Engineering for Gas Turbines and Power, Vol. 132

[24] B. Zhao, Z. Xu, X. Kan, J. Zhong, T. Guo (2016). Structural damage detection by using single natural frequency and the corresponding mode shape, Shock and Vibration

[25] M. Zhuo, L. Yang, L. Yu (2014). The steady-state thermo-mechanical analysis of turbine rotor, Applied Mechanics and Materials, Vol. 574, pp. 184--189

[26] PERMAS User's Reference Manual, INTES Publication No. 450

[27] VisPER User Manual, INTES Publication No. 470

[28] http://www.intes.de